

Zero-core-contribution model and its application to photodetachment of atomic negative ions

R. M. Stehman* and S. B. Woo

Department of Physics, University of Delaware, Newark, Delaware 19711

(Received 8 April 1977; revised manuscript received 26 March 1979)

The authors have postulated a simple physical model for atomic negative ions and have obtained general formulas to describe their photodetachment characteristics. Absolute photodetachment cross sections, accurate to a factor of 2, and the angular distributions of detached electrons are at once made available for all atomic negative ions whose l , $\langle R^2 \rangle^{1/2}$, and E are known, where l is the angular momentum quantum number for the outermost orbital electron of the anion, E and $\langle R^2 \rangle^{1/2}$ are, respectively, the electron affinity and root-mean-square radius of the neutral atom. Values of these three input parameters are readily available for most atomic anions. The model seems to encompass the major physical attributes of atomic anions required for photodetachment. Its mathematics is simple. Because of this it is suggested that the model promises applicability to more complicated systems, particularly to photodetachment from molecular negative ions, and to more complicated processes, e.g., negative-ion-neutral-atom charge exchange.

I. INTRODUCTION

The calculation of photodetachment cross sections has received considerable theoretical attention. Since the cross section for detachment of an electron depends on the matrix element for electric dipole transitions from a state describing the bound negative ion to a state of atom plus free electron, the primary task lies in obtaining an adequate representation of the initial bound and final free state. The various calculations of photodetachment cross sections can be cataloged according to the methods used to obtain the wave functions describing these states.

The existing methods can be broken into three categories, although the division between categories is not completely clear-cut. In one category are contained the calculations which use the most accurate multielectron wave functions obtainable. The calculations of Geltman¹ and Ajmera and Chung² for H⁻; of Moores and Norcross³ for various alkali-metal negative ions; of Chase and Kelly,⁴ Henry,⁵ Garrett and Jackson,⁶ and Lan *et al.*⁷ for O⁻ are all calculations employing multielectron wave functions which include polarization and/or electron correlation effects in various ways. The use of such detailed wave functions enables prediction of absolute photodetachment cross sections which are generally in good agreement with experiment, including situations in which detachment leaves the neutral atom in an excited state.

The second category contains those methods which employ only the wave function of the single electron undergoing detachment; this wave function being the solution to Schrödinger's equation with a spherically symmetric potential which describes the electron-atom interaction. Calculations of this

type have been employed by Geltman⁸ for H⁻ and Li⁻, by Klein and Brueckner⁹ for O⁻, by Cooper and Martin¹⁰ for O⁻, C⁻, Cl⁻, and F⁻, and by Robinson and Geltman¹¹ for C⁻, O⁻, F⁻, Si⁻, S⁻, Cl⁻, Br⁻, and I⁻. Typically the potential has at least one parameter which is adjusted to agree with the binding energy. This approach also yields cross sections that are in good agreement with measured cross sections.

The essential feature of the third category is the use of a bound-state wave function that describes a single electron bound by a short-range potential. In the actual calculation only the form of the wave function outside the range of the potential is used. In order to obtain this form, the electron affinity must be known. In order to calculate absolute cross sections, authors using this method have employed sum rules or have matched the asymptotic wave function to more accurate wave functions. This method has been applied to several ions for which the electron is detached from an *s*-orbital: Armstrong¹² and Adelman¹³ for H⁻ and John and Williams¹⁴ for the alkali-metal negative ions. Except for H⁻, whose neutral core is very small, phase shifts obtained from independent calculations were used as an additional set of known information.

An alternative choice of bound-state wave function which retains the computational simplicity of the third category is to use Slater orbitals. This technique has been used by Reed *et al.*¹⁵ who obtain a general formula for the relative cross sections of a wide variety of atomic negative ions. By using linear combinations of the same orbitals used for the atomic ions, these authors also did the first calculation of photodetachment cross sections for a number of diatomic and polyatomic negative ions. Their calculations give good agree-

ment with the experimental cross sections for the species considered. This agreement is accomplished by treating the coefficients in the exponents of the Slater orbitals as fitting parameters. In addition either the electron affinity must be known or is to be used as an additional fitting parameter.

Within the guidelines of our rough cataloging,¹⁶ the following pattern develops: generally, as one progresses from the first category to the last the difficulty of computation, together with the information obtained, decreases, but the number of parameters that must be specified increases. However, the accuracy of calculations obtained with all categories is about the same, except when excited states of the atom become important. In this paper we shall describe a zero-core-contribution model which leads to a method of calculating photodetachment cross sections similar to the simple technique of Armstrong¹² and Adelman,¹³ but which makes the use of phase shifts unnecessary for describing photodetachment from species whose neutral core is considerably larger than that of H⁻. In place of the final-state phase shifts used by John and Williams,¹⁴ or the fitting parameter in the exponent of the Slater original orbital used by Reed *et al.*,¹⁵ the method described here relies on knowledge of the radius of the neutral atom, which is more readily available than the phase shifts and can be determined independently of a photodetachment experiment. This radius defines a spherical core. The essential assumption of the zero-core-contribution (ZCC) model described here is that the contribution to the photodetachment cross section from inside this core region is negligible.

We have applied the method to a large variety of atomic negative ions involving detachment of either *s* or *p* orbital electrons; Secs. II and III will show that the method gives satisfactory account of the general features of the total and differential cross sections of these systems. The method estimates absolute cross sections without relying on sum rules or knowledge of more complicated wave functions. Sections IV and V discuss the nature of the approximations made by the zero-core-contribution model. The emphasis of the present work is placed on the mathematical simplicity of this method; its ability to yield a general formula for the absolute photodetachment cross sections depending on three tangible physical parameters—electron affinity, angular momentum of the outermost orbital electron, and the radius of the parent neutral atom; and its potential application to photodetachment from the diatomic and polyatomic negative ions and other processes for which the more complicated methods of computation are likely to be rather difficult.

II. METHOD FOR CALCULATING PHOTODETACHMENT CROSS SECTIONS OF ATOMS

The photodetachment cross section of a negative ion can be calculated from the dipole-length matrix element

$$\frac{d\sigma}{d\Omega} = \frac{e^2}{\hbar c} \frac{\omega k^2}{2\pi} |M_{k0}|^2, \quad (1)$$

where

$$M_{k0} = \langle k | \sum_i \hat{e} \cdot \vec{r}_i | 0 \rangle. \quad (2)$$

The state $|0\rangle$ describes the initial bound state of the negative ion and $|k\rangle$ is a state describing the neutral atom and a free electron with momentum \vec{k} . The final state is normalized to unit flux of the free electron. $d\Omega$ is an element of a solid angle, $e^2/\hbar c$ is the fine structure constant, \vec{r}_i is the coordinate of the *i*th electron, ω is the angular frequency, and \hat{e} is the direction of polarization of the incident photon.

In order to simplify the computation of the matrix element M_{k0} , we make an ansatz about the negative ion which is illustrated in Fig. 1. In this figure r_0 is a radius characteristic of the neutral atom from which the negative ion is formed. The “extra electron” is pictured as being only loosely bound to the atom, and has therefore approximately unity probability of being found outside the core. As a result of this ansatz the dipole matrix element M_{k0} coming from inside r_0 is negligible, and the major contribution to it comes from the shaded region immediately outside the core. Another ansatz is that both the wave functions of the initial and final states can be written as the product of the unperturbed atomic wave function and a one-electron wave function describing the “extra electron.” It is further assumed that the atomic wave function

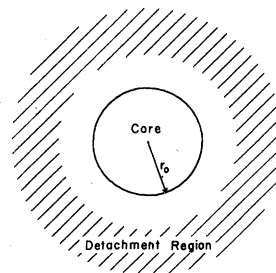


FIG. 1. Model of an atomic negative ion employed by our method of calculation. The extra electron is loosely bound by an electron-atom potential which is negligible outside the atomic radius r_0 . The loose binding allows the wave function of the extra electron to extend considerably beyond r_0 . The shaded “detachment region” represents the predominant contribution to M_{k0} .

is unchanged from the initial to the final state. Thus Eq. (2) is simplified to become

$$M_{k0} = \int_{r_0}^{\infty} \int_0^{\pi} \int_0^{2\pi} \psi_h(\vec{r}) \hat{e} \cdot \vec{r} \times \psi_0(\vec{r}) r^2 \sin\theta d\phi d\theta dr. \quad (3)$$

The radial integration extends from r_0 outwards, in keeping with our ansatz. We shall take the wave function describing the free electron to be a plane wave:

$$\psi_h(\vec{r}) = (m/\hbar k)^{1/2} e^{i\vec{k} \cdot \vec{r}}. \quad (4)$$

The wave function describing the weakly bound extra electron is assumed to be an angular momentum eigenfunction

$$\psi_0(\vec{r}) = R_l(r) Y_{lm}(\theta, \phi) \quad (5)$$

and for $r > r_0$ where the potential is assumed constant, the radial function R_l satisfies

$$\frac{1}{r^2} \frac{d}{dr} r^2 \frac{dR_l}{dr} - \frac{l(l+1)R_l}{r^2} = \gamma^2 R_l, \quad (6)$$

where $\gamma = \sqrt{2mE}/\hbar$ and E is the electron affinity. The solutions to Eq. (6) are modified spherical Bessel functions. In keeping with the zero-core-contribution assumption, the radial function R_l is normalized to one in the region outside the core:

$$\int_{r_0}^{\infty} |R_l(r)|^2 r^2 dr = 1. \quad (7)$$

We now turn to the details of the calculation of the cross section for photodetachment of an s -orbital electron, as is the case with H^- and the alkali-metal negative ions, and of a p -orbital electron as is the case with negative ions formed from elements in the third through seventh columns of the Periodic Table.

A. Detachment of an s electron

For $l=0$ the solution to Eq. (6) is

$$R_0 = Ne^{-\gamma r}/r, \quad (8)$$

with

$$N^2 = 2\gamma e^{2\gamma r_0}. \quad (9)$$

If the plane wave (4) is decomposed into partial waves, when the integration over angles is performed only the p wave survives because of the electric dipole selection rules. One obtains

$$M_{k0} = (4\pi m/\hbar k)^{1/2} i \cos\chi R_{ps} \quad (10)$$

where

$$R_{ps} = \int_{r_0}^{\infty} j_1(kr) R_0(r) r^3 dr. \quad (11)$$

Here χ is the angle between the direction of polarization \hat{e} and the momentum of the free electron \vec{k} . j_1 is the spherical Bessel function of order 1. Substituting (8) into the radial integral gives

$$R_{ps} = \frac{Ne^{-\gamma r_0}}{k^2 + \gamma^2} \left[\left(\frac{2k}{k^2 + \gamma^2} - \frac{\gamma r_0}{k} \right) \cos(kr_0) + \left(\frac{\gamma^3 + 3k^2\gamma}{k^2(k^2 + \gamma^2)} + r_0 \right) \sin(kr_0) \right]. \quad (12)$$

In terms of the quantity R_{ps} , the cross section is

$$\frac{d\sigma}{d\Omega} = \frac{2e^2}{\hbar c} \frac{m\omega k}{\hbar} \cos^2\chi R_{ps}^2. \quad (13)$$

The total cross section is obtained by integrating over all directions, χ :

$$\sigma_0 = \frac{8\pi}{3} \frac{e^2}{\hbar c} \frac{m\omega k}{\hbar} R_{ps}^2. \quad (14)$$

B. Detachment of a p electron

For $l=1$, the solution to Eq. (6) is

$$R_1 = N(e^{-\gamma r}/r)(1 + 1/\gamma r), \quad (15)$$

with

$$N^2 = 2\gamma e^{2\gamma r_0}/(1 + 2/\gamma r_0). \quad (16)$$

There are three p orbitals corresponding to $m = 0, \pm 1$. A matrix element is to be computed connecting each of these orbitals with the plane wave; the quantity $|M_{k0}|^2$ appearing in Eq. (1) is the average of the absolute squares of each of these matrix elements. When the plane wave is decomposed into partial waves and the integrations over angles performed, the selection rules pick out the s and d waves. This will leave two radial integrations which when performed give

$$R_{sp} = \frac{Ne^{-\gamma r_0}}{\gamma k(\gamma^2 + k^2)} \left[\left(\frac{3\gamma^2 k + k^3}{\gamma^2 + k^2} + \gamma k r_0 \right) \cos(kr_0) + \left(\frac{2\gamma^3}{\gamma^2 + k^2} + \gamma^2 r_0 \right) \sin(kr_0) \right] \quad (17a)$$

and

$$R_{dp} = -Ne^{-\gamma r_0} \left[\left(\frac{k^4 + 6\gamma^2 k^2 + 3\gamma^4}{\gamma k^2(\gamma^2 + k^2)^2} + \frac{r_0}{\gamma^2 + k^2} \right) \times \cos(kr_0) - \left(\frac{3}{\gamma k^3 r_0} + \frac{3k^2 + \gamma^2}{k(k^2 + \gamma^2)^2} - \frac{\gamma r_0}{k(\gamma^2 + k^2)} \right) \sin(kr_0) \right]. \quad (17b)$$

In terms of these the differential cross section is

$$\frac{d\sigma}{d\Omega} = \frac{2e^2}{9\hbar c} \frac{m\omega k}{\hbar} [\cos^2\chi (R_{sp} - 2R_{dp})^2 + \sin^2\chi (R_{sp} + R_{dp})^2] \quad (18)$$

TABLE I. Calculated σ_{\max} and the experimental σ_{\max} are compared for the detachment process which leaves the neutral atom in the ground state.

Ion	Electron affinity (eV)	r_0 (Å)	σ_{\max} Theoretical (Å ²)	σ_{\max} Experimental (Å ²)
s-orbital outermost electron				
H ⁻	0.7542	1.19	0.44	0.43 ^a
Li ⁻	0.620	2.81	1.49	1.31 ^b
Na ⁻	0.546	3.00	1.69	0.93 ^b
K ⁻	0.5012	3.65	2.41	2.44 ^b
Rb ⁻	0.486	3.84	2.66	2.60 ^b
Cs ⁻	0.4715	4.16	3.09	2.90 ^b
p-orbital outermost electron				
C ⁻	1.268	1.35	0.179	0.145 ^c
O ⁻	1.462	0.96	0.059	0.063 ^d
F ⁻	3.399	0.84	0.069	0.056 ^e
Cl ⁻	3.615	1.34	0.163	0.15 ^f
Br ⁻	3.364	1.52	0.210	0.12 ^f ; 0.23 ^g
I ⁻	3.061	1.79	0.292	0.310 ^h ; 0.21 ⁱ

^a Reference 19.

^b Reference 20.

^c Reference 22.

^d Reference 23.

^e Reference 25.

^f Reference 26.

^g Reference 27.

^h Reference 24.

ⁱ Reference 28.

and the total cross section is

$$\sigma_0 = \frac{8\pi e^2}{9\hbar c} \frac{m\omega k}{\hbar} (R_{sp}^2 + 2R_{dp}^2). \quad (19)$$

The cross sections predicted by Eqs. (18) and (19) should be multiplied by a fractional parentage coefficient of 0.3 or 0.6 when applied to anions having respectively four or five outer-shell p electrons.

III. COMPARISON WITH EXPERIMENTAL RESULTS

The electron affinity E , core radius r_0 , and angular momentum quantum number of the outer shell, l , are the three input values required for the theoretical calculations of the zero-core-contribution model. Values of l for most atomic negative ions are well known. The values of E and r_0 we employ are shown in the first two columns of Table I. The electron affinities are taken from the recent review of Hotop and Lineberger.¹⁷ The core radius r_0 is established as $r_0 = 1.3\langle R^2 \rangle^{1/2}$, where $\langle R^2 \rangle^{1/2}$ is the root-mean-square radius of the outermost occupied orbital in the neutral atom taken from Lu *et al.*¹⁸ We have taken the factor of 1.3 for all ions because it yields the best overall agreement of the calculated cross sections with experimental results. This choice implies a core region large enough to envelop almost all of the charge distribution of the neutral atoms. We now

compare calculated results with experimental results.

A. Shape of the cross section and its dependence on l , r_0 , and E

The experimental curves (dashed lines) shown in Figs. 2 and 3 clearly indicate that the angular momentum quantum number l has the primary control over the shape of the cross section. That is, the photodetachment cross section of an s -outer-shell negative ion rises to a peak and then declines, while that of a p outer shell shows a rapid rise and then levels to a plateau. The calculated results strongly reflect such a systematic dependence on l .

Examination of the experimental curves seen in Fig. 2 shows that the photodetachment cross section for s -outer-shell ions has a peak energy which shifts closer to the threshold energy for the heavier elements and that the width of the peak (FWHM) tends to narrow. The calculated results exhibit the same systematic behavior. In fact, examination of Eqs. (12) and (14) shows that the two ratios, the FWHM of the peak divided by the electron affinity, and the threshold-to-peak energy difference divided by the electron affinity, both decrease as the product γr_0 increases. Table I shows that γr_0 increases as one progresses from H⁻ to Cs⁻.

The shape of the cross section of p -orbital ions does not depend strongly on either the core radius

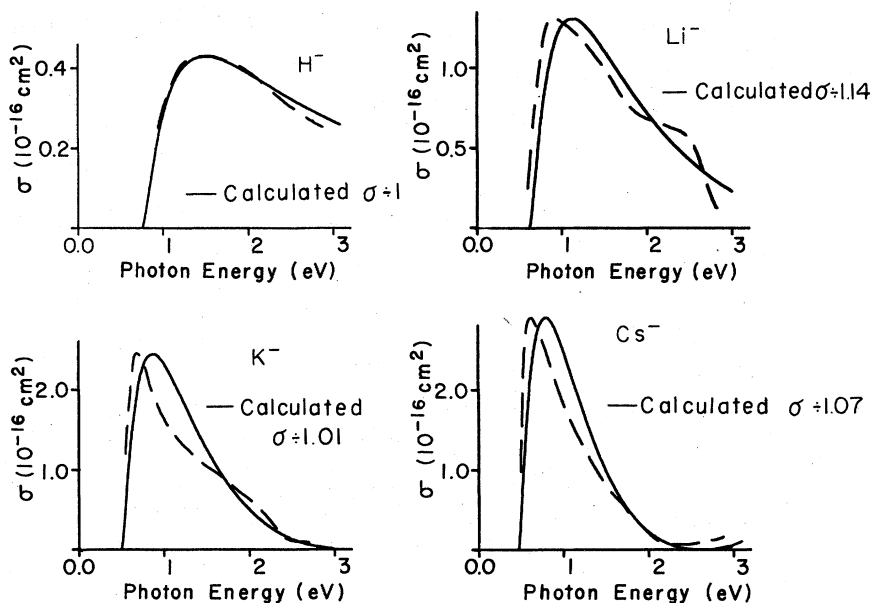


FIG. 2. Comparison of cross sections for detachment of an electron from an s orbital. The solid line shows in (a) the calculated cross section for H^- divided by a factor of 1.0; (b) the cross section for Li^- divided by 1.14; (c) that for K^- divided by 1.01; and (d) that for Cs^- divided by 1.07. The experimental cross sections are denoted by dashed lines. For H^- the experimental data is that of Smith and Burch (Ref. 19) and for the alkali metal ions is that of Kaiser *et al.* (Ref. 20).

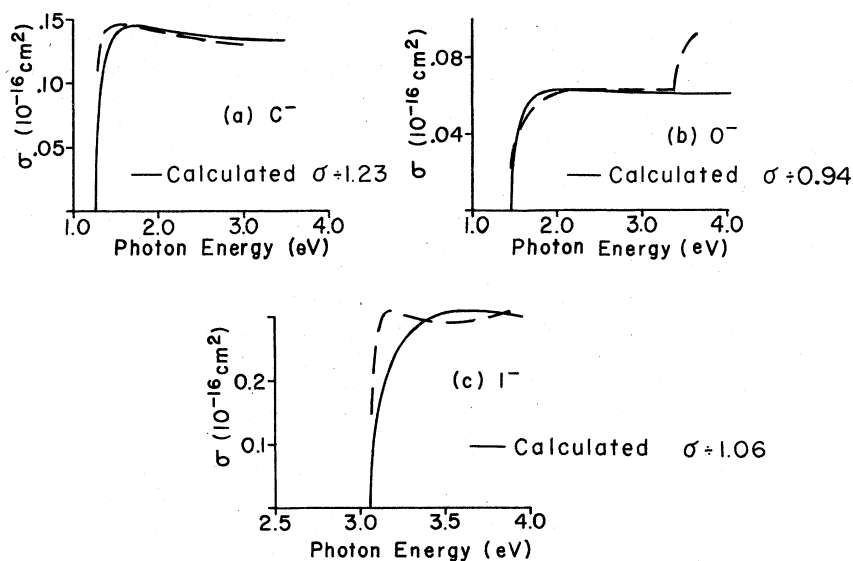


FIG. 3. Comparison of cross sections for detachment of an electron from a p orbital. The solid line in (a) shows the calculated cross section for C^- divided by 1.23; (b) shows the calculated cross section for O^- divided by 0.94; and (c) that for I^- divided by 1.06. The experimental cross sections are denoted by dashed lines. For C^- the experimental data is that of Seman and Branscomb (Ref. 22), for O^- that of Branscomb *et al.* (Ref. 23), and for I^- that of Steiner *et al.* (Ref. 24).

or the electron affinity. The theory and experiments are in qualitative agreement.

The structure which shows up as a shoulder in the Li^- experimental cross section at around 2.5 eV and in K^- at about 2.1 eV and the sharp rise in O^- cross section at around 3.4 eV are due to photodetachment leaving the neutral atom in an excited state.^{21,23} Such a photodetachment process is not accounted for by our present method which assumes that the photodetachment always leaves the neutral atom in its ground state [see discussion in Sec. IV and Eq. (26)].

Comparison of the calculated and experimental results for the shape of cross sections of Na^- and Rb^- in the s -orbital group and F^- , Cl^- , and Br^- in the p -orbital group²⁵⁻²⁸ are not shown. It suffices to state that the agreement is no worse than that shown in Figs. 2 and 3.

We also note that our calculated results fit the well-known threshold behavior²⁹

$$\sigma_0 \propto \omega k^{(2l+1)} (a_0 + a_1 k^2 + a_2 k^4 \dots) \quad (20)$$

in the limit of very small k . Here the exponent l is the smallest angular momentum allowed in the final state.

B. Peak value of the absolute cross section and its dependence on l , r_0 , and E

Examination of the last column of Table I shows that the measured peak value of the absolute photodetachment cross sections are in surprisingly good agreement with those calculated from the zero-core-contribution model. What may be more significant, however, is the way the model sorts out the systematic dependence of the peak value on l , r_0 , and E , and the order of importance of these

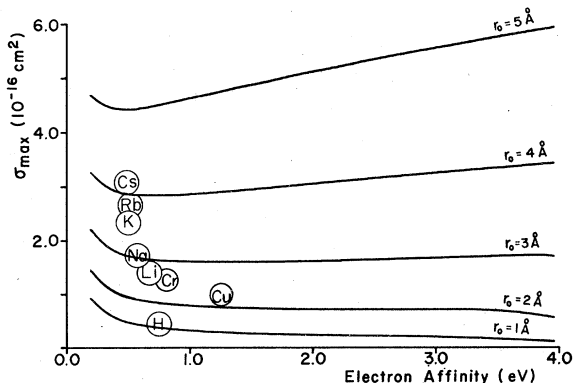


FIG. 4. Estimate of the peak amplitude of the cross section σ_{\max} can be obtained when the photodetachment process leaves the neutral atom in the ground state. Shown here is such a σ_{\max} plotted as a function of the electron affinity and the atomic radius of the neutral. This diagram is applicable only to atomic negative ions having s -orbital outermost electrons.

three variables. Figures 4 and 5 show that the theory correctly predicts that the primary dependence of the peak value is on l . That is, the peak value of the s -orbital group is in the neighborhood of 10^{-16} cm^2 , while that of the p -orbital group is about one order of magnitude smaller (see also Figs. 2 and 3). Figures 4 and 5 also show that for ions of a given l the peak value is more dependent on the core radius than the electron affinity.

Closer examination of the rightmost columns of Table I shows that excellent agreement with experimental data is obtained for all s -orbital cases, except for Na^- . Even in the case of Na^- , our value is in excellent agreement ($\pm 5\%$) with other calculated σ_{\max} .^{14,31} The agreement with experimental data for p -orbital cases³² are not as good. The calculated values tend to be larger than the experimental ones, as might be expected. Note that the electron affinity is considerably larger than 1 eV in the cases evaluated, which probably indicates that the probability of finding the additional electron inside the core is no longer insignificant. Hence the normalization factor N , calculated in accordance with the zero-core-contribution assumption, becomes artificially large.

C. Angular distribution and its dependence on l , r_0 , and E

By grouping terms, Eqs. (13) and (18) can be put in the form of

$$\frac{d\sigma}{d\Omega} = \frac{\sigma_0}{4\pi} \left[1 + \beta \left(\frac{3}{2} \cos^2 \chi - \frac{1}{2} \right) \right], \quad (21)$$

where β , the anisotropy factor, is equal to 2 for the s -orbital cases and becomes

$$\beta = 2(R_{dp}^2 - 2R_{dp}R_{sp}) / (2R_{dp}^2 + R_{sp}^2) \quad (22)$$

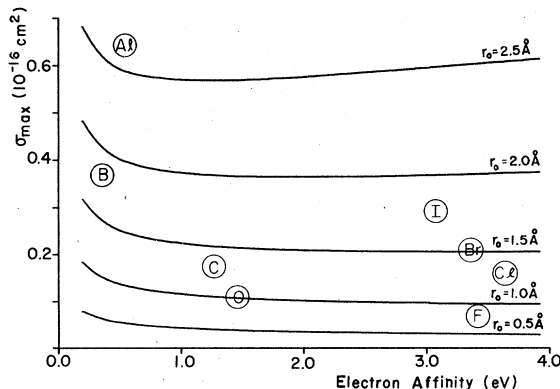


FIG. 5. This diagram is applicable only to atomic negative ions having p -orbital outermost electrons. Otherwise it is the same as Fig. 4. The σ_{\max} shown above should be multiplied by a fractional parentage coefficient of 0.3 or 0.6 when applied to anions having respectively four or five outer-shell p electrons.

for the p -orbital cases.

Theory predicts that the variable having the primary influence over the angular distribution of the photodetached electron is the angular momentum quantum number. That is, for s -orbital negative ions the differential cross section shows a pure $\cos^2\chi$ dependence regardless of r_0 , E , or the energy of the incident photon. For the p -orbital ions, the differential cross section will be uniform at photon energies slightly above the detachment threshold, and vary between uniform distribution and a $\sin^2\chi$ dependence at higher incident photon energies. One also finds that the variation of β with photon energy is more rapid for p -orbital anions of larger γr_0 .

Excellent agreement is obtained in the s -orbital cases. Experiment by Kasden and Lineberger³³ showed that $\beta=2$ within a very small experimental error for photodetachment from alkali-metal negative ions. For p -orbital cases, values of β have been measured at two different energies for C^- and at a single energy for O^- by Hall and Siegel.³⁴ Figure 6 compares calculated values with measured ones. Also included are the results computed by Cooper and Zare³⁵ using a method that employs phase shifts in the final-state calculated from a model potential. Although the calculated values in the p -orbital cases do not fall within the limits of experimental error, they have the general features of the calculated values of Cooper and Zare.

IV. JUSTIFICATION OF THE ONE-ELECTRON MODEL ASSUMING ZERO CORE

In a rigorous treatment, the photodetachment cross section is to be computed using the matrix element connecting multielectron wave functions as shown in Eq. (2). However, in the zero-core model, this matrix element is approximated by the one-electron matrix element of Eq. (3). In this section, the properties of the model which bring about this simplification are illustrated for a system in which there are two electrons participating in the detachment process. We will take both electrons to be s electrons, and their spins to be aligned so as to give a singlet state (this would correspond to H^- , or the outer shell in an alkali-metal negative ion). An analysis along similar lines for any number of electrons, with any permissible combination of orbital and spin angular momenta leads to the same conclusions reached in this simpler example.

With only two indistinguishable outer-shell electrons considered, the matrix element of Eq. (2) becomes

$$M_{h0} = \langle \phi_f(\vec{r}_1, \vec{r}_2) | \hat{e} \cdot \vec{r}_1 + \hat{e} \cdot \vec{r}_2 | \phi_i(\vec{r}_1, \vec{r}_2) \rangle. \quad (23)$$

An initial-state wave function appropriate for the

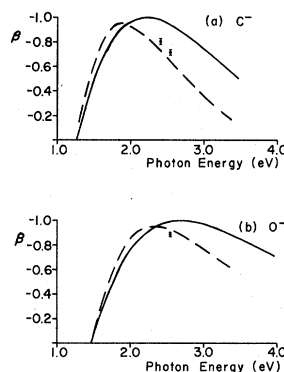


FIG. 6. Comparison of anisotropy parameter β with experiment for C^- (a) and O^- (b). The points marked \square and \times are the experimental results of Hall and Siegel (Ref. 34). The dashed lines represent the theory of Cooper and Zare (Ref. 35).

assumptions of Sec. II is

$$\phi_i(\vec{r}_1, \vec{r}_2) = \eta[\psi(\vec{r}_1)\psi_0(\vec{r}_2) + \psi_0(\vec{r}_1)\psi(\vec{r}_2)], \quad (24)$$

where ψ is the normalized wave function of the neutral atom, and ψ_0 is a normalized wave function with asymptotic behavior befitting that of an outer-shell electron of the negative ion. η represents the normalization constant, which is

$$\eta = \frac{1}{\sqrt{2}(1 + |\langle \psi | \psi_0 \rangle|^2)^{1/2}}. \quad (25)$$

The appropriate wave function for the final state is

$$\phi_f = (1/\sqrt{2})[\psi(\vec{r}_1)\psi_h(\vec{r}_2) + \psi_h(\vec{r}_1)\psi(\vec{r}_2)]. \quad (26)$$

ψ_h is the wave function representing the detached free electron. The use of ψ in Eq. (26) implies that the photodetachment always leaves the neutral atom in its ground state.

Symmetry with respect to the two-particle coordinates permits Eq. (23) to be reduced to

$$M_{h0} = 2\eta(1/\sqrt{2}) \times \{ \langle \psi | \hat{e} \cdot \vec{r} | \psi \rangle \langle \psi_h | \psi_0 \rangle + \langle \psi | \hat{e} \cdot \vec{r} | \psi_0 \rangle \langle \psi_h | \psi \rangle + \langle \psi_h | \hat{e} \cdot \vec{r} | \psi \rangle \langle \psi | \psi_0 \rangle + \langle \psi_h | \hat{e} \cdot \vec{r} | \psi_0 \rangle \langle \psi | \psi \rangle \}. \quad (27)$$

The first integral in Eq. (27), $\langle \psi | \hat{e} \cdot \vec{r} | \psi \rangle$, is zero since the neutral atom has no intrinsic dipole moment. The second integral, $\langle \psi | \hat{e} \cdot \vec{r} | \psi_0 \rangle$, is zero because of the selection rule, since the wave functions representing the two outer-shell electrons possess the same angular momentum quantum number. The third is much smaller than the fourth term, since its overlap integral, $\langle \psi | \psi_0 \rangle$, is very small compared to 1, if ψ_0 is chosen in accordance with our model. Hence

$$M_{h0} \approx \langle \psi_h | \hat{e} \cdot \vec{r} | \psi_0 \rangle, \quad (28)$$

since

$$2\eta\sqrt{2} = \sqrt{2}/(2 + 2|\langle \psi | \psi_0 \rangle|^2)^{1/2} \approx 1. \quad (29)$$

TABLE II. Comparison of moments: $\langle r^n + r_0^n \rangle$. Moments for H^- computed using a 444-parameter wave function by Pekeris (Ref. 36), an asymptotically correct 35-parameter wave function by Rotenberg and Stein (Ref. 37), an asymptotic wave function with a predetermined normalization coefficient by Adelman (Ref. 13), a Hartree-Fock calculation by Lyons *et al.* (Ref. 38), and the wave function of Eq. (24) with Eq. (8) by the zero-core model.

n	Pekeris	Rotenberg-Stein	Adelman	Hartree Fock	Zero core
1	5.42036	5.4202	5.6350	5.0078	5.9491
2	23.827	23.826	23.919	18.824	26.249
3		152.03	152.29	97.381	160.5
4		1290	1292.9	652.02	1306.7
5		13697	13720		13516

Thus the dipole matrix element reduces to an integral involving the one-electron orbitals ψ_0 and ψ_a [Eq. (3)]. In the approximation we are making, one may think of a negative ion of two indistinguishable outer-shell electrons, each giving equal contribution to photodetachment, in terms of an "equivalent" system. In this "equivalent" system, one electron occupies the outer-shell orbital of the *neutral atom* and does not contribute to photodetachment. The other electron occupies an outermost orbital described by ψ_0 , having a zero core, and is exclusively responsible for photodetachment.

The assumption that $\psi_0 = 0$ for $r < r_0$ does not imply that the charge density is small in the core region. The single-electron density resulting from the wave function of Eq. (24) is

$$\rho(r_1) = \int \phi^2(1,2) d\tau_2 = \eta^2 \{ |\psi|^2 + |\psi_0|^2 + \langle \psi | \psi_0 \rangle \psi_0^* \psi + \langle \psi_0 | \psi \rangle \psi^* \psi_0 \}. \quad (30)$$

Numerical calculation shows that this charge distribution is about 40% inside the core region for H^- , using our ψ_0 and the 1s hydrogen wave function for ψ .

Another way to test the validity of our zero-core model is to check the accuracy of moments generated from our Eq. (24) and using our zero-core wave function as ψ_0 . Such a test requires the existence of "established" moments of a negative ion to serve as standards of comparison. H^- turns out to be the only candidate since it is the only negative ion for which an accurate wave function is available for all values of r . Table II shows that the moments generated from a zero-core wave function compare quite well with those generated from the 444-parameter wave function of Pekeris³⁶ and the asymptotically correct 35-parameter wave function of Rotenberg and Stein.³⁷ The higher moments are very accurate. The first two moments, which are more related to the accuracy of the photodetachment cross section calculation than the

higher moments, are off by about 10%. Table II also shows that the moments generated from the zero-core model, despite its simplicity, are significantly better than those obtained from the standard Hartree-Fock computation.³⁸ Adelman's asymptotic approach¹³ yields accurate moments. However, his approach is not applicable to any negative ion whose normalization coefficient for the wave function is not known.

V. DISCUSSION

We believe that the simplifications of the zero-core-contribution model are inapplicable to physical processes which depend strongly on the electron-atom interaction potential, e.g., elastic scattering of electrons by neutral atoms. Another example is the absence of logarithmic terms³⁰ in our Eq. (20), since these terms arise from the long-range $1/r^4$ electron-atom interaction which is ignored in our model. The model also does not apply to physical processes which depend strongly on the wave function inside r_0 or on correlation effects, and is therefore not applicable, for example, to the calculation of electron affinities (or photodetachment cross sections when the neutral ends up in an excited final state.)

Even for a physical process for which the simplifications are ordinarily valid, such as photodetachment from atomic negative ions, the range of validity has limits. For example, (a) when the kinetic energy of the outgoing electron exceeds several electron volts, so that its deBroglie wavelength is comparable to r_0 , the contribution of the region inside r_0 is no longer negligible; (b) when the kinetic energy of the detached electron is so small that it is comparable to the electron-atom potential energy in the photodetachment region whence the differential cross section is likely to be less accurate; (c) when the electron affinity is so large that the wave function of the extra electron in the negative ion does not extend very far beyond

the radius of the neutral atom. This occurs when $1/\gamma \leq r_0$, as is the case with halogen negative ions [see Fig. 3(c)].

The apparent success of the zero-core model in the discussion of photodetachment of atomic negative ions, without the use of the phase shift, calls for some discussion. We believe that it may be derived from the combination of the following two factors. (i) The shift in phase of the outgoing wave may be small over the range of r where the photodetachment process is predominant, i.e., the shaded "detachment" region shown in Fig. 1. This certainly is the case for H^- whose total phase shift, accumulated over the entire range of r , is very small. That this may be the case for alkali-metal negative ions, whose phase shifts are large, may at first seem surprising. We note that the large phase shift of an alkali-metal negative ion is predominantly caused by its exceptionally large polarizability. The large resulting long-range polarization potential causes much of its shift in phase to occur over a range of $r \gg r_0$, where the photodetachment probability is small. The shift in phase appropriate to the detachment region is only the part of phase shift accumulated up to $r \approx r_0$, and is therefore small. (ii) The shift in phase appropriate to the detachment region is caused mostly by the short-range potential within the core. It is roughly accounted for in the zero-core model by the use of the parameters, E and r_0 . One notes the remarkable resemblance of Eq. (14) to the Bethe and Longmire formula¹² for photodestruction cross section which is

$$\sigma = \frac{32\pi}{3} \frac{e^2}{\hbar c} a_0^2 N^2 \left(\frac{k}{k^2 + \gamma^2} \right)^2 \times \left(\cos\delta + \frac{\gamma(\gamma^2 + 3k^2)}{2k^3} \sin\delta \right)^2, \quad (31)$$

where δ is the phase shift caused by the short-range potential considered in their bound-free transition. The comparison suggests that the $k r_0$ factor in the argument of the sine and cosine expression of Eq. (14) may be related to such a shift in phase.

The zero-core model has the potential weakness of assuming an unduly large core size in order to compensate for the absence of phase shifts. However, if this is the case, it should not be able to predict with equal success the photodetachment characteristics of H^- and Cs^- whose polarizability differ by about two orders of magnitude. The approximately equal degree of agreement in the cases of H^- and Cs^- shown in Fig. 2 is obtained using the same formula for the core size, namely, $r_0 = 1.3 \langle R^2 \rangle^{1/2}$. This argues against the suspicion of a big bias in our current selection of the core

size and supports the view that photodetachment calculations are not very sensitive to large phase shifts caused by the presence of long-range polarization forces.

VI. CONCLUSIONS

The zero-core-contribution model is a one-electron model. It depicts a negative ion of n indistinguishable electrons in terms of an "equivalent" system of a neutral atom and an extra electron. This extra electron has a zero-core wave function and is exclusively responsible for photodetachment. The limitations of this model are discussed in Sec. V. The accuracy of its prediction for the absolute photodetachment cross section is estimated to be better than a factor of 2. Its mathematics is simple. The results are generally applicable. It requires three input values— l , r_0 , and E . Information about these parameters are usually much more readily available than the cross sections to be calculated from this method. The size of neutral atoms are tabulated by Lu *et al.*¹⁸ A very complete list of the electron affinity of atomic negative ions is seen in Ref. 17 by Hotop and Lineberger. In the sense that the zero-core model provides general formulas whose input values are readily available, it is quite powerful. Photodetachment information, both in the form of absolute cross section and in the form of angular distribution of detached electrons are at once made available for all atomic negative ions whose value for l is zero or 1 and whose r_0 and E are known.

The model also makes the role of the major physical attributes of negative ions stand out clearly. So far as photodetachment is concerned, it shows that l has primary influence over all photodetachment characteristics, be it the shape, the peak value or the angular distribution of the cross section. The role of r_0 and E are less significant. The peak value σ_{\max} of the cross section has a moderate dependence on r_0 but is nearly independent of E . On the other hand, the shape of the cross section is influenced by the product γr_0 , where γ is proportional to \sqrt{E} .

We conjecture that the method is likely applicable to a number of processes beyond the single-photon detachment of negative atomic ions which is considered in this paper. We conceive its potential use in calculating photodetachment cross sections of diatomic and polyatomic negative ions, multiphoton detachment cross sections, negative-ion-neutral-resonant-charge-exchange cross sections at low relative energy, and negative-ion-positive-ion recombination cross sections at low relative energies.

Note added. Since this manuscript was submitted, Lamm *et al.* published an article [Phys. Rev. A **17**, 238 (1978)] which calculated the photodetachment cross section and multipole polarizability of alkali-metal anions. That article employs a mixed-zero-core method. The zero-core concept is used to determine the normalization coefficient for the bound-state wave function. However, the bound-state wave function present in the integrand in the calculation of photodetachment cross section does not have a zero core. As a result of such a mix, the values of r_0 chosen by Lamm *et al.* are approximately one-half of ours and the resulting σ_{\max} are about 0.85 to 0.9 those of ours.

In an effort to improve the final-state wave func-

tion, Lamm *et al.* incorporate a pseudopotential chosen to match phase shifts calculated by Moores and Norcross.³ It is interesting to note that if the phase shifts are arbitrarily set to zero, the σ_{\max} from their calculation decrease by only about 10%. This supports our belief that a final-state wave function with a realistic shift in phase in the "detachment region" will yield nearly the same result as obtained with a plane wave.

ACKNOWLEDGMENTS

We wish to acknowledge helpful discussions with Dr. Robert N. Hill. This work was supported in part by NSF Grant No. ATM-77-18324.

*On leave from Northeastern Illinois Univ., Chicago, Ill. 60625.

¹S. Geltman, *Astrophys. J.* **136**, 935 (1962).

²M. P. Ajmera and K. T. Chung, *Phys. Rev. A* **12**, 475 (1975).

³D. L. Moores and D. W. Norcross, *Phys. Rev. A* **10**, 1646 (1974).

⁴R. L. Chase and H. P. Kelly, *Phys. Rev. A* **6**, 2150 (1972).

⁵R. J. W. Henry, *Phys. Rev.* **162**, 56 (1967).

⁶W. R. Garrett and H. T. Jackson, *Phys. Rev.* **153**, 28 (1967).

⁷Vo Ky Lan, N. Feautrier, M. LeDourneuf, and H. van Regemorter, *J. Phys. B* **5**, 1506 (1972).

⁸S. Geltman, *Phys. Rev.* **104**, 346 (1956).

⁹M. M. Klien and K. A. Brueckner, *Phys. Rev.* **111**, 1115 (1958).

¹⁰J. W. Cooper and J. B. Martin, *Phys. Rev.* **126**, 1482 (1962).

¹¹E. J. Robinson and S. Geltman, *Phys. Rev.* **153**, 4 (1967).

¹²B. H. Armstrong, *Phys. Rev.* **131**, 1132 (1963).

¹³S. A. Adelman, *Phys. Rev. A* **5**, 508 (1972).

¹⁴T. L. John and A. R. Williams, *J. Phys. B* **5**, 1662 (1972).

¹⁵K. J. Reed, A. H. Zimmerman, H. C. Anderson, and J. I. Brauman, *J. Chem. Phys.* **64**, 1368 (1976).

¹⁶An entirely different approach from those catalogued above has been used to determine the analytic structure of the photodetachment cross section near fine-structure threshold for S^- by A. R. P. Rau and U. Fano [Phys. Rev. A **4**, 1751 (1971)] and near the threshold for leaving the neutral in excited state for Cs^- by C. M. Lee [Phys. Rev. A **11**, 1692 (1975)]. While this approach does not require knowledge of the initial or final wave functions, it is intended to yield information about the cross section only over narrow energy regions.

¹⁷H. Hotop and W. C. Lineberger, *J. Phys. Chem. Ref. Data* **4**, 539 (1975).

¹⁸C. C. Lu, T. A. Carlson, F. B. Malik, T. C. Tucker, and C. W. Nestor, Jr., *At. Data* **3**, 1 (1971).

¹⁹S. J. Smith and D. S. Burch, *Phys. Rev.* **116**, 1125

(1959).

²⁰H. J. Kaiser, E. Heinicke, R. Rackwitz, and D. Feldman, *Z. Phys.* **270**, 259 (1974).

²¹T. A. Patterson, H. Hotop, A. Kasdan, D. W. Norcross, and W. C. Lineberger, *Phys. Rev. Lett.* **32**, 189 (1974).

²²M. L. Seman and L. M. Branscomb, *Phys. Rev.* **125**, 1602 (1962).

²³L. M. Branscomb, S. J. Smith, and G. Tisone, *J. Chem. Phys.* **43**, 2906 (1965).

²⁴B. Steiner, *Phys. Rev.* **173**, 136 (1968); B. Steiner, M. L. Seman and L. M. Branscomb, in *Atomic Collision Processes*, edited by M. R. C. McDowell (North-Holland, Amsterdam, 1962), p. 557.

²⁵A. Mandl, *Phys. Rev. A* **3**, 251 (1971).

²⁶R. S. Berry, C. W. Reimann and G. N. Spokes, *J. Chem. Phys.* **37**, 2278 (1962).

²⁷H. Frank, M. Neiger, and H. P. Popp, *Z. Naturforsch.* **A 25**, 1617 (1970).

²⁸A. Mandl and H. A. Hymann, *Phys. Rev. Lett.* **31**, 417 (1973).

²⁹cf. L. M. Branscomb, in *Atomic and Molecular Processes*, edited by D. R. Bates (Academic, New York, 1962), p. 105.

³⁰T. F. O'Malley, L. Spruch, and L. Rosenberg, *J. Math. Phys.* **2**, 491 (1961).

³¹D. W. Norcross and D. L. Moores, in *Atomic Physics 3*, edited by G. K. Walters and S. J. Smith (Plenum, New York, 1973), p. 261.

³²B. Steiner, in *Case Studies in Atomic and Molecular Physics II*, edited by E. W. McDaniel and M. R. C. McDowell (North-Holland, Amsterdam, 1972), p. 483.

³³A. Kasdan and W. C. Lineberger, *Phys. Rev. A* **10**, 1658 (1974).

³⁴J. L. Hall and M. W. Siegel, *J. Chem. Phys.* **48**, 943 (1968).

³⁵J. Cooper and R. N. Zare, *J. Chem. Phys.* **48**, 942 (1968).

³⁶C. L. Pekeris, *Phys. Rev.* **126**, 1470 (1962).

³⁷M. Rotenberg and J. Stein, *Phys. Rev.* **182**, 1 (1969).

³⁸D. Lyons, P. W. Langhoff, and R. P. Hurst, *Phys. Rev.* **151**, 60 (1966).